

# Examination Of Structural Morphological and Magnetic Behaviour of ZnFe<sub>2</sub>O<sub>4</sub> Nanoparticle Synthesised by Co-Precipitation Method

C. Sambathkumar, S. Ezhil Arasi, B. Natarajan, A. Arivarasan, P. Devendran



**Abstract**— The Zinc Ferrites (ZnFe<sub>2</sub>O<sub>4</sub>) nanoparticles (NPs) successfully synthesized by co-precipitation method. As prepared NPs were annealed with different temperature at 800 and 1000 °C. The crystalline phase, surface morphology and elemental distribution were confirmed by XRD, SEM and EDS respectively. The prepared ZnFe<sub>2</sub>O<sub>4</sub> XRD pattern confirm the cubic crystalline nature. The surface morphology of the prepared sample was found irregular rock like structure due to ferric metal. FTIR, EDS studies prove characteristics behavioural vibration of Zn-Fe-O elements and purity of the sample correspondingly. Prepared ZnFe<sub>2</sub>O<sub>4</sub> sample exhibit a super paramagnetic nature with the saturated magnetization of 22.066 emu/g and coercivity of 15 Oe by VSM analysis.

**Keywords:** Zinc-ferrite NPs, Co-precipitation, High-density magnetic storage media, Super paramagnetic.

## I. INTRODUCTION

Nanoparticles intense from current interest in basic scientific studies to miniaturization of devices, as well as verity of applications in energy storage devices [1-2] magnetic storage media [3], medicine [4-6] and bio-sensing and sensing [7-11]. Depending upon the physical properties differ intensely from their bulk complements rising behind their small size. In a particular manner, magnetic nanoparticles (MNPs) from their smaller size, non-toxicity, inject ability, biocompatibility and high leveling in biomedical applications [12, 13]. Transition metal oxides and metal sulfides are extensively studied due to their verity of potential applications [14-17]. Among them, the binary metal oxide shows the peculiar properties due to the combination of two elements and doping effect, by this way the binary metal oxides having applications in multidisciplinary area [18]. Recently, Binary magnetic oxides materials are becoming trendy materials for multifunctional applications in different

Along with various materials, particularly spinel-ferrite structured (XFe<sub>2</sub>O<sub>4</sub>, X=Zn, Ni, Co, Bi, etc.) materials are admired magnetic materials for different applications due to

peculiar properties such as, electric generators, inductor coils, transformer, recorder, nano fluids and bio-medical applications. Moreover, spinel- ferrite structures are more feasible with cost-effectively [18]. Zinc ferrite is an essential material for widely used magnetic materials and these spinel-ferrite structured materials have good photocatalytic properties. In addition, the catalyst can be easily isolate by applying magnetic field for catalyst reusability [19]. Zinc ferrite structured materials suggested an enhanced displaying with attractive photo sensitivity in narrow band width of ~1.9 eV for photocatalytic applications [20].

Here, we employed zinc ferrite (ZnFe<sub>2</sub>O<sub>4</sub>) NPs by co-precipitation method and confirmed with different studies like structural, morphological and magnetic behaviors. The prepared ZnFe<sub>2</sub>O<sub>4</sub> sample exhibits a super paramagnetic nature.

## II. MATERIAL SYNTHESIS

### A. Chemicals

All reagents were used with A.R grade was used. Zinc nitrate (Zn(NO<sub>3</sub>)<sub>2</sub>•6H<sub>2</sub>O), Iron nitrate (Fe(NO<sub>3</sub>)<sub>3</sub>) and Sodium hydroxide (NaOH) were purchased from sigma Aldrich. The solvents ethanol and De-ionized water were performed for entire reaction.

### B. Synthesis method

In this typical synthesis co-precipitation method was adapted for Zinc ferrite NPs synthesis. Equal molar ratio of (Zn(NO<sub>3</sub>)<sub>2</sub>•6H<sub>2</sub>O), as precursors and NaOH as alkaline medium. The process in co-precipitation reaction involves three major steps, they are, nucleation, growth, coarsening and agglomeration process. When the precipitation process starts, the nucleation occurs simultaneously. After that they form an aggregation which makes the particles to become quite higher size nanoparticles and thermodynamically stable. This is followed by the coarsening in which formed particles grow further to produce nanoparticles.

The ferrite nanoparticles were formed by co-precipitation and ferritisation processes. The base medium converts the metal salts into hydroxides. On heating the formed hydroxides, the nanoparticles get transformed into ferrite but it takes some time in co-precipitation method. Hence the precipitate was collected and washed extensively with ethanol dried in hot oven for 7 h.

Manuscript published on 30 December 2019.

\* Correspondence Author (s)

P. Devendran<sup>\*</sup>, [p.devendran@klu.ac.in](mailto:p.devendran@klu.ac.in), [pdevavenmani@gmail.com](mailto:pdevavenmani@gmail.com)

<sup>a</sup>Department of Physics, International Research Centre, Kalasalingam Academy of Research and Education, Krishnankoil – 626126, Tamil Nadu, India.

<sup>b</sup>Department of chemistry, SRM institute of science and technology, Kattankulathur, Chennai, Tamilnadu

© The Authors. Published by Blue Eyes Intelligence Engineering and Sciences Publication (BEIESP). This is an [open access](https://creativecommons.org/licenses/by-nc-nd/4.0/) article under the CC-BY-NC-ND license <http://creativecommons.org/licenses/by-nc-nd/4.0/>.

### C. Characterization Technique

The prepared nanoferrite samples were characterized with Powder XRD by Rigaku Miniflex II X-ray Diffractometer. The XRD patterns were recorded with CuK $\alpha$  monochromatic radiation (1.5406 Å). The morphology and elemental analysis were analyzed using the FEI-QUANTA-FEG 250 (SEM) equipped with EDX analyzer. The Shimadzu IR Trace-100 spectrometer was employed to find functional groups presence in zinc ferrite NPs with the help of KBr pellet system. The magnetic nature of prepared ZnFe<sub>2</sub>O<sub>4</sub> NPs was carried out in a vibrating sample magnetometer (VSM) Lake Shore is having an electromagnet capable of delivering fields up to 1.5 Tesla. The magnetometer is able to detect magnetic moments down to 10<sup>-6</sup> emu, at room temperature.

## III. RESULTS AND DISCUSSION

### A. Powder XRD Analysis

The phase composition of phases and crystal structure of samples was analyzed by powder X-ray diffraction. The Fig. 1 shows, as prepared sample exhibited amorphous nature. Further, the sample was calcined with different temperature at 800 °C and 1000 °C. After calcination clear broad peaks was appeared and all the diffraction peaks are closely coincides with cubic structured zinc ferrite crystalline structure (JCPDS card No. 74-2397) in this 2 $\theta$  range 29.9, 35.26, 36.84, 42.8, 53.09, 56.59 and 62.1 with corresponding hkl planes (220), (311), (222), (400), (422), (511) and (440) respectively.

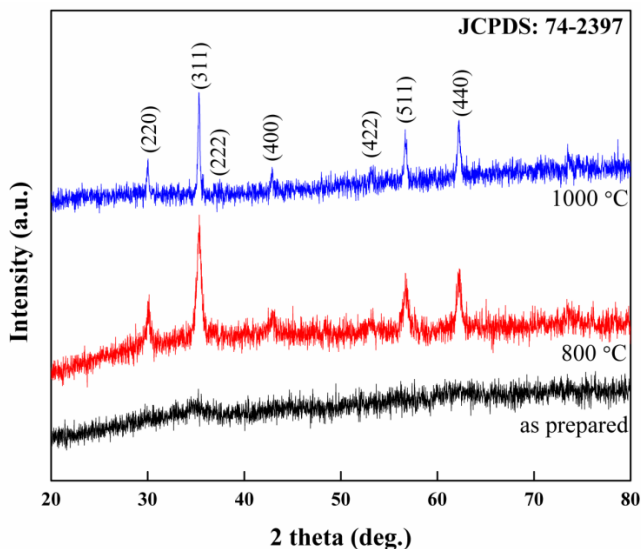


Fig. 1. XRD Pattern Of (a) ZnFe<sub>2</sub>O<sub>4</sub>, calcined ZnFe<sub>2</sub>O<sub>4</sub> at (b) 800 °C and 1000 °C nanoparticles.

This all crystalline peaks which were confirmed the formation of zinc ferrite NPs. The XRD pattern of zinc ferrite nanoparticles calcined at 800 °C shows the emergence of few peaks of zinc ferrite indicating the origin of crystalline phase. This can also be done through examining the XRD pattern of the prepared nanoparticles calcined at 1000 °C. Further increase in calcination temperature to 1000 °C increased the sharpness of the peaks [15,18,21]. The sharp peaks good indicated the size increment and crystallinity.

### B. FTIR analysis

The formation of spinel ZnFe<sub>2</sub>O<sub>4</sub> structure in the pure Fig. 2.(a) and calcined zinc ferrite nanoparticles Fig. 2.(b-c) was further confirmed by FT-IR spectrum. The FTIR spectrum of zinc ferrite samples is shown in Fig. 2. The peaks at 550 cm<sup>-1</sup> and 680 cm<sup>-1</sup> was due to the stretching vibration of metal-oxygen (Fe-O) bond interaction and it also shows the formation of spinel structure in zinc ferrite compound. The spectra showed a strong band at 433 cm<sup>-1</sup> and 1082 cm<sup>-1</sup> which is a characteristic of Zn-O vibrational band. The stretching vibration between Zn-O-Fe bonds were ascribed in two bands at 1355 cm<sup>-1</sup> and 860 cm<sup>-1</sup>. The broad absorption at 3400-3600 cm<sup>-1</sup> corresponds to the O-H stretching vibrations [15, 18].

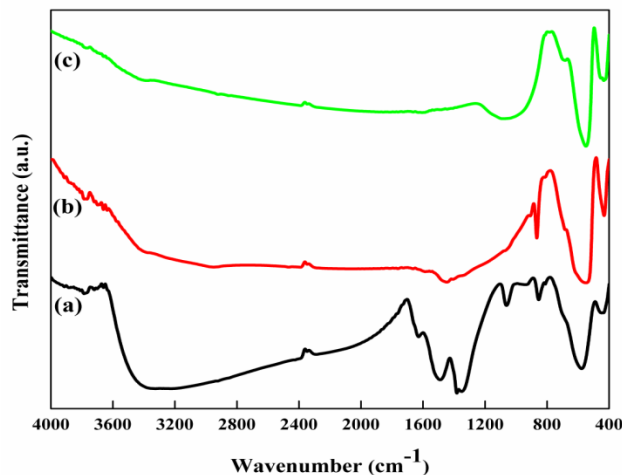


Fig. 2. FTIR spectra of (a) as prepared (b) calcined at 800 °C and (c) calcined at 1000 °C ZnFe<sub>2</sub>O<sub>4</sub> nanoparticles.

### C. Surface and Elemental analysis

Fig. 3. reveals the morphology of the zinc ferrite nanoparticles calcined at different temperature. The SEM images of ZnFe<sub>2</sub>O<sub>4</sub> sample reveals irregular shape particles with different magnifications all the particles are appeared rock like structures due to Fe ions. No major particle size was obtained in pure and calcined samples. The surface morphology of all the samples are observed from SEM analysis 20 nm to few micro meter ranges due to agglomeration and irregular shape.

An EDX spectrum reveals the purity and elemental composition of the ZnFe<sub>2</sub>O<sub>4</sub> NPs. Fig 3. (b), (d) and (f) shows, the EDX pattern of synthesized ZnFe<sub>2</sub>O<sub>4</sub> samples and the heat-treated samples. Elemental concentration obtained all three samples is given in Table. I. EDX confirmed the formation and purity of the presence chemical constituents such as oxygen (O), zinc (Zn), and iron (Fe) elements [18].

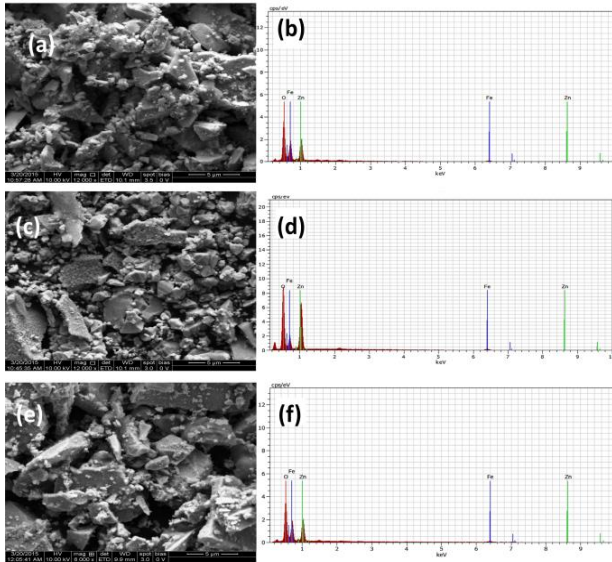


Fig. 3. (a, c, e) SEM images of as prepared ZnFe<sub>2</sub>O<sub>4</sub> NPs with different calcination temp. 800 and 1000 °C and (b, d, f) EDX spectra of corresponding samples.

The fig 3(c) shows that the elemental composition of the prepared composite. The carbon contains the peak at the K $\alpha$  radiation characteristic x-ray emit at the range of 0.277keV and the intensity was high. It shows the moreover the percentage of carbon was very high from the EDAX graph 38.1%. The Oxygen exhibits the range of radiation characteristic x-ray K $\alpha$  0.525keV and the oxygen contain 33.5%. Finally, the Ni peak contains in the range of 7.47keV in 28.4%.

TABLE I. ELEMENTAL ANALYSIS OF ZINC FERRITE NANOPARTICLES

Temperature	As prepared		800°C		1000°C	
	Weight %	Atomic %	Weight %	Atomic %	Weight %	Atomic %
O	40.80	69.72	38.43	70.20	42.02	73.21
Zn	30.40	13.61	31.69	14.17	29.45	12.55
Fe	28.80	16.67	29.88	15.64	28.53	14.24
Total	100.0	100.0	100.0	100.0	100.0	100.0

#### D. VSM Analysis

The magnetic properties of the calcined at 1000°C ZnFe<sub>2</sub>O<sub>4</sub> NPs was determined by VSM. Fig. 4 show the magnetic field dependence of magnetization (M-H) of ZnFe<sub>2</sub>O<sub>4</sub> NPs measured at ambient temperature (300 K) with an expanded scale of the low field in the insets. The saturated magnetization and coercivity of the sample are tabulated in Table. II. From the Hysteresis loop ZnFe<sub>2</sub>O<sub>4</sub> sample was exhibit a superparamagnetic nature with the saturated magnetization of 22.066 emu/g and coercivity of 15 Oe, respectively [18]. The sample gets magnetized with the applied field and when the field is increased the magnetization also increased and vice-versa. Their coercive fields (H<sub>c</sub>) are almost negligible which indicate the sample exhibits the super paramagnetic behavior and it is clearly signifying the insert image. The biocompatible magnetic nanoparticles may play an important role in biomedical applications.

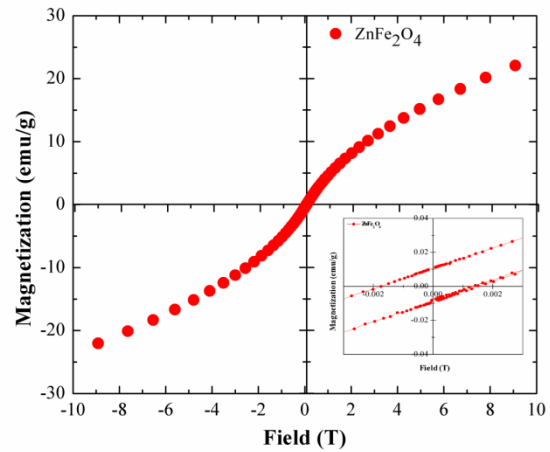


Fig. 4. Magnetic Hysteresis Loops of ZnFe<sub>2</sub>O<sub>4</sub> nanoparticles calcined at 1000 °C

TABLE II. MAGNETIC PROPERTIES OF ZINC FERRITE NANOPARTICLES CALCINED AT 1000°C.

Samples	Coercivity (T)	Saturation magnetization (emu/g)
ZnFe <sub>2</sub> O <sub>4</sub>	0.00150	22.066

#### IV. CONCLUSION

The Zinc Ferrite NPs have been successfully prepared via co-precipitation technique. The base medium was used for the reaction with the help of aqueous sodium hydroxide. The as prepared ZnFe<sub>2</sub>O<sub>4</sub> NPs were annealed at two different annealing temperatures 800°C and 1000°C. The crystalline phases, functional groups and surface morphology of the samples were evaluated using XRD, FTIR, SEM and EDX respectively. XRD spectra confirmed the formation of zinc ferrite nanoparticles. On maximizing the annealing temperature, the diffracted peaks became sharper and decreased intensity and peak width. It clearly proves that, increase the crystallinity at high temperature. The FTIR spectra showed a strong band at 433cm<sup>-1</sup> and 1082cm<sup>-1</sup> which is characteristic of Zn-O vibrational band. From the SEM analysis, the surface morphology consists of irregular shapes and the particles size was found 20 nm to few micrometer range. The existence of elements and their percentage was analyzed by EDX which confirmed the presence of chemical constituents such as oxygen (O), zinc (Zn) and Iron (Fe) elements. VSM analysis of ZnFe<sub>2</sub>O<sub>4</sub> nanoparticles have confirmed the superparamagnetic nature at room temperature with a saturation magnetization of 22 emu/g respectively with coercive forces 0.0015 T. ZnFe<sub>2</sub>O<sub>4</sub> nanoparticles can be considered as potential materials for various applications. Thus developed method can be a potential method to obtain biocompatible ZnFe<sub>2</sub>O<sub>4</sub> nanoparticles for wide spectrum of applications particularly in biomedical field.

# Examination of structural morphological and magnetic behaviour of ZnFe<sub>2</sub>O<sub>4</sub> nanoparticle synthesised by co-precipitation method

## ACKNOWLEDGMENT

Author C. Sambathkumar gratefully thank Kalasalingam Academy of Research and Education(KARE) to provide University Research Fellowship scheme and besides thankful to IRC for provide research facilities.

## REFERENCES

1. N. Sattarahmady, A. Parsa, H. Heli, "Albumin nanoparticle-coated carbon composite electrode for electrical double-layer biosupercapacitor applications". *J. Mater. Sci.* 48, 2346–2351 (2013).
2. H. Heli, H. Yadegari, A. Jabbari, "Investigation of the Lithium Intercalation Behavior of Nanosheets of LiV<sub>3</sub>O<sub>8</sub> in an Aqueous Solution". *J. Phys. Chem.* 115C, 10889–10897 (2011).
3. S. Sun, C.B. Murray, D. Weller, L. Folks, A. Moser, "Monodisperse FePt nanoparticles and ferromagnetic FePt nanocrystal superlattices". *Science* 287, 1989–1992 (2000).
4. H. Heli, S. Mirtorabi, K. Karimian, "Advances in iron chelation: an update". *Expert Opin. Ther. Pat.* 21, 819–856 (2011).
5. R. Lehner, X. Wang, M. Wolf, P. Hunziker, "Designing switchable nanosystems for medical application". *J. Control Release* 161, 307–316 (2012).
6. P. Boisseau, B. Loubaton, "Nanomedicine, Nanotechnology in medicine". *C. R. Phys.* 12, 620–636 (2011).
7. A. Rahi, K. Karimian, H. Heli, "Nanostructured materials in electroanalysis of pharmaceuticals". *Anal. Biochem.* 497, 39–47 (2016).
8. N. Sattarahmady, H. Heli, R. Dehdari Vais, "An electrochemical acetylcholine sensor based on lichen-like nickel oxide nanostructure". *Biosens. Bioelectron.* 48, 197–202 (2013).
9. A. Rahi, N. Sattarahmady, H. Heli, "Label-free electrochemical aptasensing of the human prostate-specific antigen using gold nanospears". *Talanta* 156–157, 218–224 (2016).
10. A. Rahi, N. Sattarahmady, H. Heli, "Zepto-molar electrochemical detection of Brucella genome based on gold nanoribbons covered by gold nanoblooms". *Sci. Rep.* 5, 18060 (2015).
11. N. Sattarahmady, G.H. Tondro, M. Golchin, H. Heli, "Gold nanoparticles biosensor of Brucella spp. genomic DNA: Visual and spectrophotometric detections". *Biochem. Eng. J.* 97, 1–7 (2015).
12. A.A.M. Elsherbini, M. Saber, M. Aggag, A. El-Shahawy, H.A. Shokier, "Magnetic nanoparticle-induced hyperthermia treatment under magnetic resonance imaging". *Magn. Reson. Imaging* 29, 272–280 (2011).
13. H. Heli, N. Sattarahmady, G.R. Hatam, F. Reisi, R. Dehdari Vais, "An electrochemical genosensor for Leishmania major detection based on dual effect of immobilization and electrocatalysis of cobalt-zinc ferrite quantum dots". *Talanta* 156–157, 172–179 (2016).
14. P. Devendran, T. Alagesan, T. R. Ravindran, K. Pandian, "Synthesis of spherical CdS quantum dots using cadmium diethyldithiocarbamate as single source precursor in olive oil medium". *Current Nanoscience*, 2014, 10, 302-307.
15. K. Ravichandran, R. Mohan, B. Sakthivel, S. Varadharajaperumal, P. Devendran, T. Alagesan, K. Pandian, "Enhancing the photocatalytic efficiency of sprayed ZnO thin films through double doping (Sn + F) and annealing under different ambiances". *Applied Surface Science*, 2014, 321, 310-317.
16. P. Devendran, T. Alagesan, A. Manikandan, S. Asath Bahadur, M. Krishna Kumar, S. Rathinavel, K. Pandian, "Sonochemical Synthesis of Bi<sub>2</sub>S<sub>3</sub> Nanowires using Single Source Precursor and Study of Its Electrochemical Activity". *Nanoscience and Nanotechnology Letters*, 2016, 8, 1-6.
17. A. Shameem, P. Devendran, V. Siva, M. Raja, A. Manikandan, S. Asath Bahadur, "Preparation and Characterization of Nanostructured CdO thin films by SILAR method for Photocatalytic Application". *Journal of inorganic and organometallic polymers and materials*, 2017, 27, 692–699.
18. M. G. Naseri, E. B. Saion, A. Kamali, "An Overview on Nanocrystalline ZnFe<sub>2</sub>O<sub>4</sub>, MnFe<sub>2</sub>O<sub>4</sub>, and CoFe<sub>2</sub>O<sub>4</sub> Synthesized by a Thermal Treatment Method". *ISRN Nanotechnology*, vol. 2012, 604241, pp 1-11, 2012. <https://doi.org/10.5402/2012/604241>.
19. S. Sun, X. Yang, Y. Zhang, F. Zhang, J. Ding, J. Bao, C. Gao, "Enhanced photocatalytic activity of sponge-like ZnFe<sub>2</sub>O<sub>4</sub>

synthesized by solution combustion method". *Progress in Natural Science: Materials International*, 22, 6, 2012, 639–643.

20. X.Y. Li, Y. Hou, Q.D. Zhao, L.Z. Wang A general, "one-step and template-free synthesis of sphere-like zinc ferrite nanostructures with enhanced photocatalytic activity for dye degradation". *Journal of Colloid and Interface Science*, 358 (2011), pp. 102-108.
21. K. Maaz, S. Karim, A. Mumtaz, S. K. Hasanain, J.Liu, J. L.Duan, "Synthesis and magnetic characterization of nickel ferrite nanoparticles prepared by co-precipitation route". *Journal of Magnetism and Magnetic Materials*, 321, 12, 2009, 1838-1842.